Conclusion

Our spectroscopic evidence indicates that the major (porphinato)manganese species produced upon oxygen transfer to (tetraarylporphinato)manganese(III) complexes contain monomeric manganese(IV) centers. These complexes are $S = {}^3/_2$ spin systems and exhibit negative hyperfine shifts in their low-temperature ^2H NMR spectra. Although our spectroscopic data do not support the presence of manganese(V) complexes, we cannot discount its presence at minute concentrations in our low-temperature reaction products.

In the absence of a sixth coordinating ligand such as 4-Mepy, equilibrium concentrations of manganese(III) porphyrin π-cation radical likely react with chlorine atoms (present from homolytic bond cleavage of Cl_2 or OCl_2) to afford a reactive isoporphyrin. This complex is structurally analogous to an electrochemically produced isoporphyin but is considerably more reactive. The reactive metalloisoporphyrin effectively executes oxidative chlorination and allylic oxidation of cyclohexene. Thus, this complex is likely the species or at least one of the species responsible for the poor epoxide specificity observed in the absence of nitrogen donor ligands in the catalytic hypochlorite oxidation system.

Acknowledgment. Financial support from National Science Foundation Grant CHE 87-05703 is gratefully acknowledged. Gratitude is expressed to Professor Charles Schultz for helpful discussions regarding the ESR spectra of these complexes.

Registry No. Mn[(*N*-CH_3)TPP]Cl, 59765-80-9; 4-Mepy, 108-89-4; cyclohexene, 110-83-8; iodide, 20461-54-5.

Cubic, Butterfly, and Oxygen-Capped Clusters of *n*-Butyloxotin Phosphinates. A New Class of Organotin Compounds[1,2]

Robert R. Holmes,* K. C. Kumara Swamy, Charles G. Schmid,[3] and Roberta O. Day

Contribution from the Department of Chemistry, University of Massachusetts, Amherst, Massachusetts 01003. *Received February 26, 1988*

Abstract: Reaction of *n*-butylstannoic acid with the phosphinic acids, R_2PO_2H, where R = *tert*-butyl, benzyl, and cyclohexyl, has led to new types of structural forms for hexacoordinated tin: two cubic clusters, $[n\text{-BuSn(O)O}_2\text{P}(t\text{-Bu})_2]_4$ (**1**) and $[n\text{-BuSn(O)O}_2\text{P(CH}_2\text{Ph})_2]_4$ (**2**), respectively, and a "butterfly" cluster, $[n\text{-BuSn(OH)(O}_2\text{P(C}_6\text{H}_{11})_2)_2]_2$ (**3**). Interesting transformations of cubes and the butterfly derivative yield oxygen-capped cluster formulations, $[(R'\text{Sn(OH)O}_2\text{PR}_2)_3\text{O}][R_2PO_2]$, where R′ = *n*-Bu and R = C_6H_{11} or CH_2Ph. ^{119}Sn and ^{31}P NMR show these structural characteristics in solution. The ^{119}Sn chemical shift correlates with increasing cluster complexity, i.e., with an increasing ligand to tin component in the various formulations discovered so far. **1** crystallizes in the triclinic space group $P\bar{1}$ with a = 13.616 (4) Å, b = 13.857 (3) Å, c = 20.544 (4) Å, α = 79.95 (2)°, β = 69.16 (2)°, γ = 71.15 (2)°, and Z = 2. **2** crystallizes in the tetragonal space group $P\bar{4}2_1c$ with a = 17.630 (4) Å, c = 11.825 (3) Å, and Z = 2. **3** crystallizes in the triclinic space group $P\bar{1}$ with a = 10.758 (3) Å, b = 12.133 (4) Å, c = 13.038 (4) Å, α = 79.93 (2)°, β = 73.72 (2)°, γ = 89.53 (2)°, and Z = 1. The conventional unweighted residuals were 0.038 (**1**), 0.042 (**2**), and 0.042 (**3**).

Our recent discovery of new structural forms of oxotin derivatives from the reaction of *n*-butylstannoic acid with phosphinic acids[1b,2,4-6] prompts us to explore the versatility of this reaction with regard to the range of possible products and their accompanying interconversions.

The reaction of monoorganostannoic acids with carboxylic acids has led to the formation of "drum" $[R'\text{Sn(O)O}_2\text{CR}]_6$[7-9] and "open-drum" (or "ladder") $[(R'\text{Sn(O)O}_2\text{CR})_2R'\text{Sn(O}_2\text{CR})_3]_2$[8,9] compositions. With phosphinic acids, a greater variety of

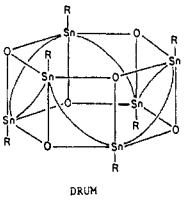

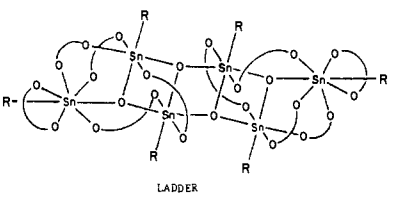

structures has been found. Although, the open-drum arrangement has yet to be observed, previous work has revealed phosphinic acids taking part in the formation of the mixed-drum composition, $[(\text{MeSn(O)O}_2\text{CMe})(\text{MeSn(O)O}_2\text{P}(t\text{-Bu})_2)]_3$,[1b] the cube formulation, $[n\text{-BuSn(O)O}_2\text{P(C}_6\text{H}_{11})_2]_4$,[4] and an oxygen-capped cluster unit, $[(n\text{-BuSn(OH)O}_2\text{PPh}_2)_3\text{O}][\text{Ph}_2\text{PO}_2]$.[5] A schematic of the latter unit illustrates its structural relationship with the drum formulation. When diphenylphosphoric acid is reacted in place of diphenylphosphinic acid, a drum $[n\text{-BuSn(O)O}_2\text{P(OPh)}_2]_6$[1b]

(1) (a) Organotin Clusters. 4. (b) Part 3: Day, R. O.; Chandrasekhar, V.; Kumara Swamy, K. C.; Holmes, J. M.; Burton, S. D.; Holmes, R. R. *Inorg. Chem.* **1988**, *27*, 2887-2893.

(2) Kumara Swamy, K. C.; Schmid, C. G.; Burton, S. D.; Nadim, H.; Day, R. O.; Holmes, R. R. *Abstracts of Papers*, 195th National Meeting of the American Chemical Society, Toronto, Canada, June 1988; American Chemical Society: Washington, DC, 1988; Abstract INOR 508.

(3) This work represents in part a portion of the Ph.D. Thesis of C. G. S., University of Massachusetts, Amherst, MA.

(4) Kumara Swamy, K. C.; Day, R. O.; Holmes, R. R. *J. Am. Chem. Soc.* **1987**, *109*, 5546-5548.

(5) Day, R. O.; Holmes, J. M.; Chandrasekhar, V.; Holmes, R. R. *J. Am. Chem. Soc.* **1987**, *109*, 940-941.

(6) Holmes, R. R.; Day, R. O.; Chandrasekhar, V.; Schmid, C. G.; Holmes, J. M. *Abstracts of Papers*, 193rd National Meeting of the American Chemical Society, Denver, CO, April 1987; American Chemical Society: Washington, DC, 1987; Abstract INOR 385.

(7) Chandrasekhar, V.; Day, R. O.; Holmes, R. R. *Inorg. Chem.* **1985**, *24*, 1970-1971.

(8) Holmes, R. R.; Schmid, C. G.; Chandrasekhar, V.; Day, R. O.; Holmes, J. M. *J. Am. Chem. Soc.* **1987**, *109*, 1408-1414.

(9) Chandrasekhar, V.; Schmid, C. G.; Burton, S. D.; Holmes, J. M.; Day, R. O.; Holmes, R. R. *Inorg. Chem.* **1987**, *26*, 1050-1056.

0002-7863/88/1510-7060$01.50/0

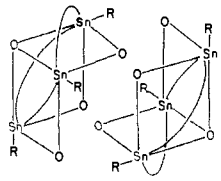

O-CAPPED CLUSTER

is obtained. The latter product results under reflux in benzene. When this reaction with *n*-butylstannoic acid is conducted at 25 °C, the oxygen-capped cluster $[(n\text{-BuSn(OH)O}_2\text{P(OPh)}_2)_3\text{O}][(\text{PhO})\text{PO}_2]$ forms.[1b] These two derivatives have been shown to interconvert reversibly. An interconversion also has been established in the case of drum and ladder compounds, e.g., between $[n\text{-BuSn(O)O}_2\text{CC}_6\text{H}_{11}]_6$ and $[(n\text{-BuSn(O)O}_2\text{CC}_6\text{H}_{11})_2(n\text{-BuSn(O}_2\text{CC}_6\text{H}_{11})_3)]_2$.[9]

These results suggest that other transformations between different geometrical forms are possible. It is noted that the stoichiometry of stannoic acid to phosphorus-based acid increases from 1:1 in the reaction yielding a drum to 1:$^4/_3$ for the reaction giving the O-capped cluster.[1b] The cube would have the same stoichiometric relation to the O-capped cluster. Structurally, it is more related than the drum to the latter, suggesting a possible interconversion may exist here as well.

In this work, the reaction of *n*-butylstannoic acid with phosphinic acids provides hexacoordinated tin in the cubic environments, $[n\text{-BuSn(O)O}_2\text{P}(t\text{-Bu})_2]_4$ (**1**) and $[n\text{-BuSn(O)O}_2\text{P(CH}_2\text{Ph})_2]_4$ (**2**), and in a new geometrical form characterized as a "butterfly" representation, $[n\text{-BuSn(OH)(O}_2\text{P(C}_6\text{H}_{11})_2)_2]_2$ (**3**). All are new compounds. Their X-ray structures are reported, and a study of their ^{119}Sn NMR spectra shows that both **2** and **3** undergo transformations in solution to oxygen-capped clusters.

Experimental Section

Chemicals were obtained from Aldrich, Fisher Scientific, and Alfa and used without further purification. Methylstannoic acid was prepared according to the procedure given by Lambourne.[10] Di-*tert*-butylphosphinic acid[11] and dicyclohexylphosphinic acid[12] were prepared by literature methods. A sample of dibenzylphosphinic acid was provided by Professor L. D. Quin. *n*-Butylstannoic acid was a gift from the Koriyama Kasei Co., Ltd., and was purified by using excess KOH in $CHCl_3$ to remove a small amount of $n\text{-BuSn(OH)Cl}_2$ and/or $n\text{-BuSn(OH)}_2\text{Cl}$ suspected[9] as a contaminant. Solvents used were of HPLC grade (Fisher Scientific). Further purification was done according to standard procedures.[13]

^{1}H, ^{31}P, and ^{119}Sn NMR spectra (proton decoupled) were recorded on a Varian X-L 300 FT/NMR spectrometer equipped with a multinuclear broad-band probe and operated at 300, 121.4, and 11.862 MHz, respectively. Resonances are referenced vs tetramethylsilane (^{1}H), tetramethyltin (external standard,^{119}Sn), and 85% orthophosphoric acid (external standard, ^{31}P). Infrared spectra were recorded by using KBr windows on a Perkin-Elmer Model 180 spectrometer.

Tetrameric *n*-Butyloxotin Di-*tert*-butylphosphinate, $[n\text{-BuSn(O)O}_2\text{P}(t\text{-Bu})_2]_4$ (1). *n*-Butylstannoic acid (0.774 g, 3.71 mmol) was allowed to react with di-*tert*-butylphosphinic acid (0.585 g, 3.70 mmol) in benzene (100 mL) under reflux for 9 h. *Caution*! Benzene is a class A carcinogen and should be used in a well-ventilated hood. Azeotropic removal of the water formed in the reaction was achieved with a Dean–Stark apparatus. Evaporation of the solvent yielded a white solid. Recrystallization from CH_2Cl_2/hexane gave mostly large, clear crystals and a small amount of white solid. Both had the same melting point; mp 364–366 °C (total yield 1.11 g, 86%). ^{31}P NMR (C_6D_6; ppm): 62.6 (s, with ^{119}Sn satellites, $^2J(^{31}\text{P–O–}^{119}\text{Sn})$ = 125 Hz). ^{119}Sn NMR (C_6D_6; ppm): −473.0 (t, $^2J(^{119}\text{Sn–O–}^{31}\text{P})$ = 128 Hz, $^2J(^{119}\text{Sn–O–}^{117}\text{Sn})$ = 170 Hz). IR (Nujol; cm^{-1}): 1085, ν_{POO}(asym) 1000, ν_{POO}(sym) 609, 554, ν_{SnO}; 489, ν_{SnC}. Anal. Calcd for $C_{12}H_{27}O_3PSn$: C, 39.05; H, 7.39. Found: C, 39.06; H, 7.27.

Tetrameric *n*-Butyloxotin Dibenzylphosphinate, $[n\text{-BuSn(O)O}_2\text{P(CH}_2\text{C}_6\text{H}_5)_2]_4$ (2). The procedure was similar to that used for **1**. Reagents and conditions: *n*-butylstannoic acid (1.05 g, 5 mmol), dibenzylphosphinic acid (1.23 g, 5 mmol); solvent, toluene (70 mL); reaction time, 2 h. The compound was crystallized from a dichloromethane/hexane/methanol/diethyl ether mixture (30 mL, 4:2:1:1 by volume). **2** was obtained as beautiful multifaceted crystals, mp 150–154 °C (yield 0.6 g, 23%). ^{1}H NMR of the cube ($CDCl_3$; ppm): 7.40–7.00 (br, aromatic), 3.05–2.80 (sextuplet or ddd; CH_2–Ph), 1.70–0.70 (*Bu*–Sn). ^{119}Sn NMR ($CDCl_3$; ppm): −464.4 (t, $^2J(Sn\text{–O–}P)$ = 111.4 Hz). ^{31}P NMR ($CDCl_3$; ppm): 49.64 (s, with ^{119}Sn satellites, $^2J(Sn\text{–O–}P)$ = 109 Hz). Anal. Calcd for $C_{72}H_{92}O_{12}P_4Sn_4$: C, 49.46; H, 5.27. Found: C, 49.51; H, 5.24.

A ^{119}Sn NMR spectrum taken immediately upon solution of the cube **2** in $CDCl_3$ showed only the triplet centered at −464.4 ppm. As a function of time, an additional triplet at −499.2 ppm, ^2J(Sn–O–P) = 130.9 Hz, grew in. The percent intensity assigned to the lower and upper field peaks, respectively, changed as follows: 1 h, 70:30; 3 h, 50:50; 4 h, 35:65; 7.5 h, 18:82. The ^{31}P NMR spectrum reflected a similar percent change with time. ^{31}P NMR ($CDCl_3$; ppm): 48.64 (^2J(Sn–O–P) = 127.4 Hz).

Dimeric *n*-Butylhydroxytin Bis(dicyclohexylphosphinate), $[n\text{-BuSn(OH)(O}_2\text{P(C}_6\text{H}_{11})_2)_2]_2$ (3) (Preparation A), and Tetrameric *n*-Butyloxotin Dicyclohexylphosphinate, $[n\text{-BuSn(O)O}_2\text{P(C}_6\text{H}_{11})_2]_4$ (5). The procedure was similar to that adapted for **2** with the same molar quantities of reagents. During the workup after removal of toluene, diethyl ether was added to induce precipitation. Recrystallization was carried out with a dichloromethane/hexane (2:1) mixture. Slow evaporation of the solvent at 20 °C yielded the first crop of crystals, which contained small arrow-shaped crystals, **5** (mp 263–265 °C; yield 0.28 g, 14% based on stannoic acid used), and larger multifaceted crystals, **3** (mp 220–223 °C; yield 0.02 g, 1%). Compounds **3** and **5** could be easily separated by handpicking. ^{119}Sn NMR ($CDCl_3$; ppm) for **3**: −547.47 [dt, ^2J(Sn–O–P) (bridging) = 128 Hz, ^2J(Sn–O–P) (dangling) = 182 Hz]. ^{31}P NMR ($CDCl_3$; ppm) for **3**: 56.02 (s, with ^{119}Sn satellites, ^2J(Sn–O–P) = 124.4 Hz (bridging)), 47.60 (s, with ^{119}Sn satellites, ^{2}J(Sn–O–P) = 190.8 Hz (dangling)). The ratio of the intensities of these two ^{31}P NMR signals was 1:1. Anal. Calcd for $C_{56}H_{108}O_{10}P_4Sn_2$: C, 51.64; H, 8.30. Found: C, 50.90; H, 8.19. X-ray analysis was performed on crystals from this preparation.

Compound **3** undergoes a slow structural change in chloroform solution. The final product **4** has the following NMR data. ^{119}Sn NMR ($CDCl_3$; ppm): −497.80 (t, ^2J(Sn–O–P) = 132 Hz). ^{31}P NMR ($CDCl_3$; ppm): 54.56 (^2J(Sn–O–P) = 129.0 Hz).

Preparation B. *n*-Butyltin trichloride (0.845 g, 3.00 mmol) and silver dicyclohexylphosphinate (3.3 g, 9.8 mmol) were reacted together in dry chloroform (60 mL) under reflux for 3.5 h. Filtration of the silver salts yielded a gold-colored filtrate. Evaporation of the filtrate under a stream of dry nitrogen and subsequent recrystallization attempts from methylene chloride, hexane, and finally diethyl ether, gave a crop of clear crystals of **3**, mp 224–228 °C (yield 50 mg, 3% based on $n\text{-BuSnCl}_3$). ^{119}Sn NMR (C_6D_6; ppm): −547.8 [dt, ^2J(Sn–O–P) (bridging) = 121 Hz, ^2J(Sn–O–P) (dangling) = 172 Hz]. ^{31}P NMR (C_6D_6; ppm): 55.6 (s, with ^{119}Sn satellites, ^2J(Sn–O–P) = 121 Hz (bridging), 46.8 (s, with ^{119}Sn satellites, ^2J(Sn–O–P) = 172 Hz (dangling)). The lattice constants on a crystalline sample were identical with those from preparation A.

Transformation of Tetrameric *n*-Butyloxotin Dicyclohexylphosphinate, $[n\text{-BuSn(O)O}_2\text{P(C}_6\text{H}_{11})_2]_4$ (5), to the Oxygen-Capped Cluster $[(n\text{-BuSn(OH)O}_2\text{P(C}_6\text{H}_{11})_2)_3\text{O}][(\text{C}_6\text{H}_{11})_2\text{PO}_2]$ (4). The synthesis and structural characterization of **5**, X-ray analysis, and ^{119}Sn NMR have been reported.[4] Additional data are the following. ^{31}P NMR ($CDCl_3$; ppm): 55.9 (^2J(Sn–O–P) = 114 Hz). In the same preparation that was reported for **5** (yield 0.8 g, 20%),[4] additional workup of the mother liquor resulted in the isolation of a second solid, **4** (yield 2.0 g, 48%) identified by its NMR spectra. ^{119}Sn NMR ($CHCl_3$; ppm): −499.5 (^2J(Sn–O–P) = 132 Hz). ^{31}P NMR ($CHCl_3$; ppm) (main peaks): 54.7 (^2J(Sn–O–P) = 128 Hz), 44.0 (free phosphinate $(C_6H_{11})_2PO_2^-$). The ratio of the integrals of these two was 3.6:1. An additional small peak was observed at ≈+56 ppm.

X-ray Studies. All X-ray crystallographic studies were done with an Enraf-Nonius CAD4 diffractometer and graphite-monochromated molybdenum radiation (λ(Mo Kα) = 0.71073 Å) at an ambient temperature of 23 ± 2 °C. Details of the experimental procedures have been described previously.[14]

Crystals were mounted in thin-walled glass capillaries, which were sealed as a precaution against moisture sensitivity. Data were collected by the θ–2θ scan mode with $3° \le 2\theta_{\text{Mo K}\alpha} \le 43°$ for **1** and $3° \le 2\theta_{\text{Mo K}\alpha} \le 50°$ for **2** and **3**. The structures were solved by use of Patterson and difference Fourier techniques and were refined by full-matrix least squares.[15]

(10) Lambourne, H. *J. Chem. Soc.* **1922**, *121*(2), 2533–2540.
(11) Mason, G. W.; Lewey, S. *J. Inorg. Nucl. Chem.* **1974**, *36*, 911–915.
(12) Peppard, D. F.; Mason, G. W.; Andrejasich, C. M. *J. Inorg. Nucl. Chem.* **1965**, *27*, 697–709.
(13) Vogel, A. I. *Textbook of Practical Organic Chemistry*; Longman: London, 1978.
(14) Sau, A. C.; Day, R. O.; Holmes, R. R. *Inorg. Chem.* **1981**, *20*, 3076–3081.

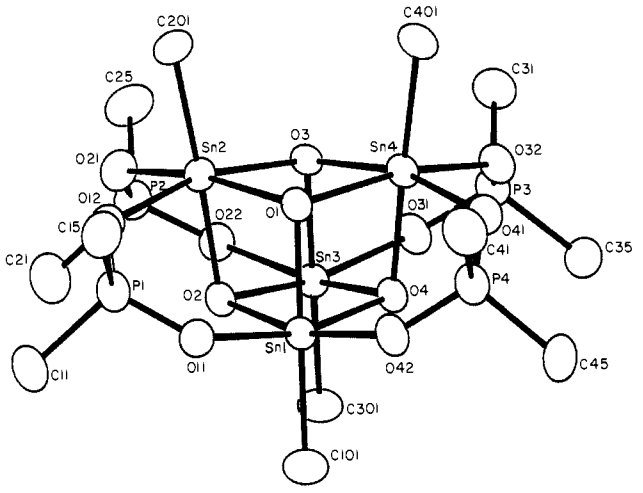

Figure 1. ORTEP plot of $[n\text{-BuSn(O)O}_2\text{P}(t\text{-Bu})_2]_4$ (**1**) with thermal ellipsoids at the 35% probability level. Pendant carbon atoms are omitted for purposes of clarity.

All computations were performed on a Microvax II computer with the Enraf-Nonius SDP system of programs.

X-ray Study for $[n\text{-BuSn(O)O}_2\text{P}(t\text{-Bu})_2]_4$ (1). The crystal used for the X-ray study was cut from a large colorless chunky crystal and had dimensions of 0.25 × 0.28 × 0.30 mm.

Crystal Data: $[n\text{-BuSn(O)O}_2\text{P}(t\text{-Bu})_2]_4$ (**1**), triclinic space group $P\bar{1}$-C_i^1 (No. 2),[16] a = 13.616 (4) Å, b = 13.857 (3) Å, c = 20.544 (4) Å, α = 79.95 (2)°, β = 69.16 (2)°, γ = 71.15 (2)°, Z = 2, and $\mu_{\text{Mo K}\alpha}$ = 1.59 mm^{-1}. A total of 7794 independent reflections ($+h,\pm k,\pm l$) was measured. No corrections were made for absorption.

The 68 independent non-hydrogen atoms were refined anisotropically. Hydrogen atoms were omitted from the refinement. The final agreement factors[17] were R = 0.038 and R_w = 0.058 for the 6652 reflections having $I \geq 2\sigma_I$.

X-ray Study for $[n\text{-BuSn(O)O}_2\text{P(CH}_2\text{Ph})_2]_4$ (2). A polyfaceted colorless crystal having maximum dimensions of 0.25 × 0.38 × 0.40 mm was used for the X-ray study.

Crystal Data: $[n\text{-BuSn(O)O}_2\text{P(CH}_2\text{Ph})_2]_4$ (**2**), tetragonal space group $P\bar{4}2_1c$-D_{2d}^4 (No. 114),[18] a = 17.630 (4) Å, c = 11.825 (3) Å, Z = 2, and $\mu_{\text{Mo K}\alpha}$ = 1.49 mm^{-1}. A total of 1884 independent reflections ($+h,+k,+l$; $|h| \geq |k|$) was measured. No corrections were made for absorption.

Of the 23 independent non-hydrogen atoms, 20 were refined anisotropically. The three pendant carbon atoms of the n-Bu group (C2–C4) were located only with difficulty and were refined isotropically. The 14 independent benzyl group hydrogen atoms were included in the refinement in idealized positions (riding) with fixed isotropic thermal parameters set at 1.3 times the equivalent isotropic B for the bonded carbon atom. Butyl group hydrogen atoms were omitted from the refinement. The final agreement factors[17] were R = 0.042 and R_w = 0.053 for the 1522 reflections having $I \geq 2.5\sigma_I$.

X-ray Study for $[n\text{-BuSn(OH)(O}_2\text{P(C}_6\text{H}_{11})_2)_2]_2$ (3). The crystal used for the X-ray study was cut from a large colorless chunk and had dimensions of 0.25 × 0.35 × 0.45 mm.

Crystal Data: $[n\text{-BuSn(OH)(O}_2\text{P(C}_6\text{H}_{11})_2)_2]_2$ (**3**), triclinic space group $P\bar{1}$-C_i^1 (No. 2),[16] a = 10.758 (3) Å, b = 12.133 (4) Å, c = 13.038 (4) Å, α = 79.93 (2)°, β = 73.72 (2)°, γ = 89.53 (2)°, Z = 1, and $\mu_{\text{Mo K}\alpha}$ = 0.926 mm^{-1}. A total of 5626 independent reflections ($+h,\pm k,\pm l$) was measured. No corrections were made for absorption.

The 36 independent non-hydrogen atoms were refined anisotropically. The 22 independent hydrogen atoms of the cyclohexyl groups bonded to P2 were treated as described for **2**. The hydroxyl hydrogen atom was located on a difference Fourier map and was included in the refinement as a fixed isotropic scatterer. The structural parameters for the associated carbon atoms did not support inclusion of the remaining hydrogen atoms in calculated positions, and these hydrogen atoms were omitted from the refinement. The final agreement factors[17] were R = 0.042 and

(15) The function minimized was $\sum w|F_o| - |F_c|)^2$, where $w^{1/2} = 2F_oLp/\sigma_I$. Mean atomic scattering factors were taken from: Reference 16, 1974; Vol. IV, pp 72–98. Real and imaginary dispersion corrections were taken from the same source, pp 149–150.

(16) *International Tables for X-ray Crystallography*; Kynoch: Birmingham, England, 1969; Vol. I, p 75.

(17) $R = \sum w||F_o| - |F_c||/\sum|F_o|$ and $R_w = |\sum w(|F_o| - |F_c|)^2/\sum w|F_o|^2|^{1/2}$. For **2**, these values are for the configuration having the lowest R_w.

(18) Reference 16, p 204.

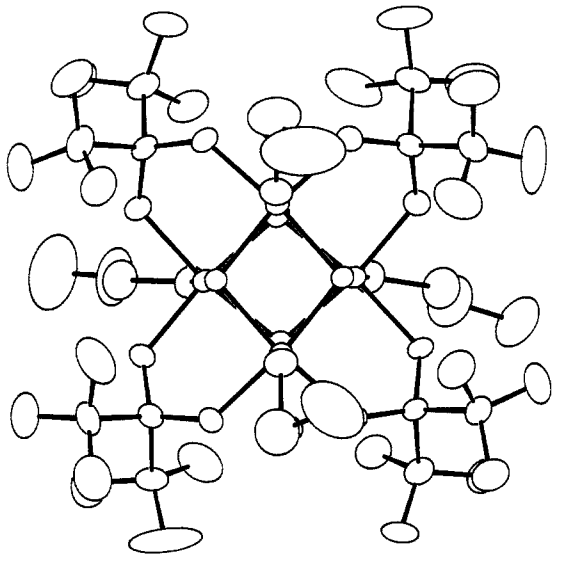

Figure 2. ORTEP plot of $[n\text{-BuSn(O)O}_2\text{P}(t\text{-Bu})_2]_4$ (**1**) with thermal ellipsoids at the 35% probability level. The view is down the pseudo S_4 axis.

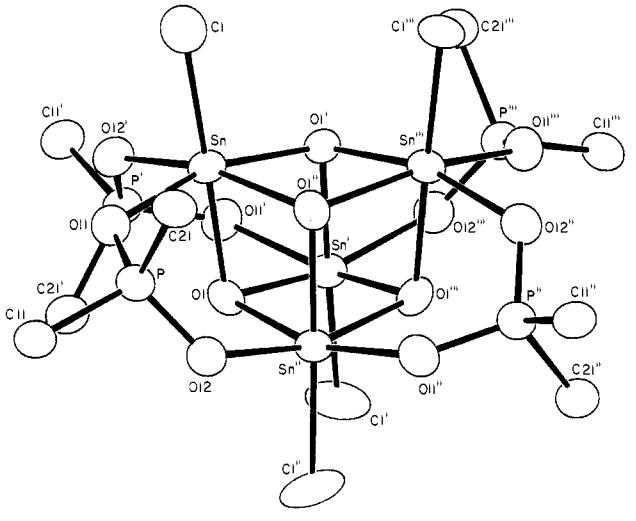

Figure 3. ORTEP plot of $[n\text{-BuSn(O)O}_2\text{P(CH}_2\text{Ph}_2)_2]_4$ (**2**) with thermal ellipsoids at the 35% probability level. Hydrogen atoms and the following carbon atoms are omitted for purposes of clarity: phenyl groups C12–C17 (C12 bonded to C11) and C22–C27 (C22 bonded to C21); pendant atoms of the n-Bu groups C2–C4 (C2 bonded to Cl). Symmetry operators: primed = $y, -x, -z$; double primed = $-y, x, -z$; triple primed = $-x, -y, z$.

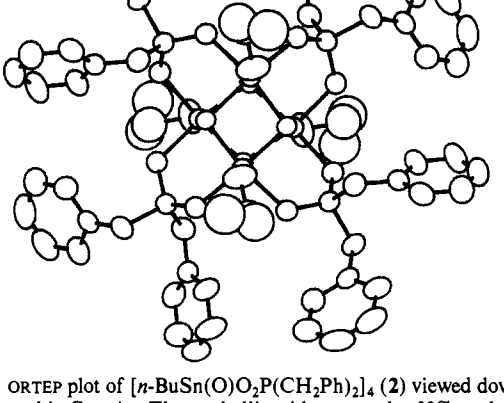

Figure 4. ORTEP plot of $[n\text{-BuSn(O)O}_2\text{P(CH}_2\text{Ph})_2]_4$ (**2**) viewed down the crystallographic S_4 axis. Thermal ellipsoids are at the 50% probability level. Hydrogen atoms are omitted for purposes of clarity.

Table I. Atomic Coordinates in Crystalline $[n\text{-BuSn(O)O}_2\text{P}(t\text{-Bu})_2]_4$ (**1**)[a]

atom[b]	x	y	z	B_{eq}[c]	atom[b]	x	y	z	B_{eq}[c]
Sn1	0.25407 (4)	0.30143 (3)	0.32850 (2)	2.91 (1)	C27	0.4426 (9)	−0.0554 (9)	0.0924 (7)	11.3 (4)
Sn2	0.28869 (4)	0.23255 (3)	0.17953 (2)	2.87 (1)	C28	0.349 (1)	−0.1903 (7)	0.1380 (6)	9.1 (4)
Sn3	0.35111 (4)	0.06130 (3)	0.29531 (2)	2.90 (1)	C31	0.7119 (7)	−0.1040 (6)	0.1922 (4)	4.9 (2)
Sn4	0.49802 (4)	0.21477 (3)	0.22741 (2)	2.95 (1)	C32	0.6931 (9)	−0.2119 (7)	0.2017 (6)	7.5 (3)
P1	0.0757 (2)	0.4324 (1)	0.2457 (1)	3.64 (5)	C33	0.6812 (9)	−0.0435 (8)	0.1292 (5)	7.0 (3)
P2	0.2435 (2)	0.0068 (1)	0.1884 (1)	3.72 (5)	C34	0.8356 (8)	−0.1135 (8)	0.1792 (6)	7.3 (3)
P3	0.6199 (2)	−0.0286 (2)	0.2684 (1)	3.64 (5)	C35	0.6632 (6)	−0.0688 (7)	0.3475 (4)	5.2 (2)
P4	0.4455 (2)	0.4011 (2)	0.3298 (1)	3.89 (5)	C36	0.6911 (9)	−0.1864 (8)	0.3637 (5)	7.9 (3)
O1	0.3460 (3)	0.3218 (3)	0.2252 (2)	2.9 (1)	C37	0.7589 (7)	−0.0286 (9)	0.3412 (5)	7.8 (3)
O2	0.2208 (3)	0.1917 (3)	0.2841 (2)	2.9 (1)	C38	0.5637 (8)	−0.0193 (9)	0.4080 (5)	7.6 (3)
O3	0.4279 (3)	0.1192 (3)	0.1969 (2)	2.8 (1)	C41	0.4556 (7)	0.5271 (6)	0.2836 (5)	5.1 (2)
O4	0.3984 (3)	0.1764 (3)	0.3238 (2)	2.9 (1)	C42	0.371 (1)	0.6147 (8)	0.3268 (9)	14.8 (7)
O11	0.1243 (4)	0.4223 (3)	0.3039 (2)	3.6 (1)	C43	0.439 (1)	0.5270 (8)	0.2153 (6)	11.4 (4)
O12	0.1363 (4)	0.3497 (3)	0.1932 (2)	3.5 (1)	C44	0.5727 (9)	0.5390 (9)	0.2642 (8)	10.8 (4)
O21	0.2322 (4)	0.1173 (4)	0.1589 (2)	4.0 (1)	C45	0.4814 (6)	0.3723 (7)	0.4108 (4)	5.3 (2)
O22	0.3012 (4)	−0.0274 (3)	0.2432 (2)	3.7 (1)	C46	0.4703 (9)	0.2637 (8)	0.4380 (5)	9.4 (3)
O31	0.5078 (4)	−0.0466 (3)	0.2860 (3)	3.7 (1)	C47	0.5994 (8)	0.3692 (9)	0.3984 (6)	8.2 (3)
O32	0.6222 (4)	0.0818 (3)	0.2481 (3)	3.8 (1)	C48	0.402 (1)	0.451 (1)	0.4670 (5)	10.5 (4)
O41	0.5268 (4)	0.3191 (3)	0.2799 (2)	3.7 (1)	C101	0.1603 (7)	0.2748 (6)	0.4363 (4)	4.8 (2)
O42	0.3258 (4)	0.4027 (4)	0.3502 (3)	4.1 (1)	C102	0.0970 (9)	0.3705 (7)	0.4782 (5)	6.9 (3)
C11	−0.0655 (6)	0.4205 (6)	0.2868 (5)	4.9 (2)	C103	0.039 (1)	0.346 (1)	0.5540 (6)	9.4 (4)
C12	−0.1064 (7)	0.3983 (8)	0.2313 (5)	7.4 (3)	C104	−0.050 (1)	0.307 (1)	0.5610 (8)	15.8 (7)
C13	−0.1462 (8)	0.5153 (8)	0.3263 (6)	7.3 (3)	C201	0.3533 (6)	0.2754 (6)	0.0708 (4)	4.4 (2)
C14	−0.0567 (8)	0.3292 (7)	0.3413 (6)	7.8 (3)	C202	0.2609 (9)	0.3110 (9)	0.0332 (5)	7.5 (3)
C15	0.0847 (7)	0.5573 (6)	0.1954 (4)	4.9 (2)	C203	0.299 (1)	0.360 (1)	−0.0363 (6)	11.5 (3)
C16	0.0152 (8)	0.5872 (8)	0.1460 (5)	7.0 (3)	C204	0.197 (1)	0.407 (1)	−0.0600 (7)	13.3 (6)
C17	0.2063 (8)	0.5398 (7)	0.1515 (5)	6.5 (3)	C301	0.2729 (6)	0.0002 (6)	0.3975 (4)	4.2 (2)
C18	0.0489 (8)	0.6411 (6)	0.2456 (5)	6.6 (3)	C302	0.2925 (8)	−0.1161 (6)	0.4058 (5)	5.8 (3)
C21	0.1027 (6)	−0.0045 (6)	0.2300 (5)	5.5 (2)	C303	0.241 (1)	−0.1586 (9)	0.4773 (7)	10.0 (5)
C22	0.0383 (8)	0.040 (1)	0.1788 (7)	13.1 (5)	C304	0.148 (2)	−0.114 (1)	0.514 (1)	19.7 (8)
C23	0.1037 (9)	−0.1150 (8)	0.2571 (8)	10.6 (5)	C401	0.6067 (6)	0.2549 (6)	0.1273 (4)	4.4 (2)
C24	0.0549 (9)	0.060 (1)	0.2904 (8)	11.7 (4)	C402	0.7212 (7)	0.2483 (7)	0.1301 (5)	6.4 (3)
C25	0.3287 (7)	−0.0753 (6)	0.1142 (4)	5.1 (2)	C403	0.7945 (8)	0.272 (1)	0.0552 (7)	10.4 (4)
C26	0.279 (1)	−0.047 (1)	0.0544 (5)	12.6 (5)	C404	0.903 (1)	0.263 (2)	0.051 (1)	17.6 (8)

[a] Numbers in parentheses are estimated standard deviations. [b] Atoms are labeled to agree with Figures 1 and 2. [c] Equivalent isotropic thermal parameters are calculated as $^4/_3[a^2\beta_{11} + b^2\beta_{22} + c^2\beta_{33} + ab(\cos\gamma)\beta_{12} + ac(\cos\beta)\beta_{13} + bc(\cos\alpha)\beta_{23}]$.

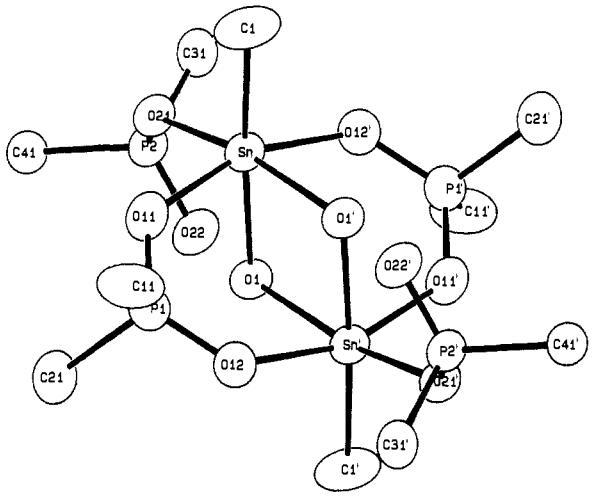

Figure 5. ORTEP plot of $[n\text{-BuSn(OH)(O}_2\text{P(C}_6\text{H}_{11})_2)_2]_2$ (**3**) with thermal ellipsoids at the 35% probability level. Hydrogen atoms and pendant carbon atoms are omitted for purposes of clarity. Primed atoms are related to unprimed ones by $-x, -y, -z$.

$R_w = 0.061$ for the 4890 reflections having $I \geq 2\sigma_I$.

Results

The atom-labeling scheme for **1** is given in the ORTEP plots of Figures 1 and 2. Atomic coordinates are given in Table I, and selected bond lengths and angles are given in Table II. The corresponding information for **2** and **3** is given in Figures 3–6 and in Tables III–VI. Thermal parameters and additional bond lengths and angles for **1**–**3** and hydrogen atom parameters for **2** and **3** are provided as supplementary material.

Discussion

Synthetic Aspects and Transformations. Although the butterfly cluster **3** was prepared by both reaction of *n*-butylstannoic acid

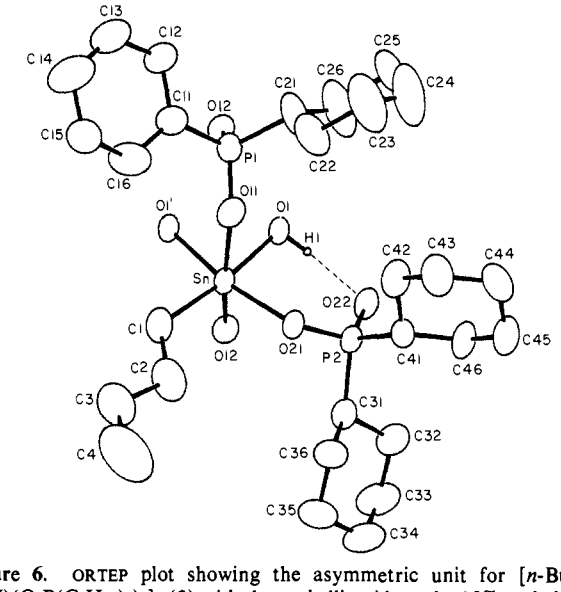

Figure 6. ORTEP plot showing the asymmetric unit for $[n\text{-BuSn(OH)(O}_2\text{P(C}_6\text{H}_{11})_2)_2]_2$ (**3**) with thermal ellipsoids at the 35% probability level. Hydrogen atoms, except for H1, are omitted for purposes of clarity. The hydrogen-bonding interaction is indicated by a dashed line. A symmetry-related O1 is shown to complete the coordination sphere of the Sn atom.

with the appropriate phosphinic acid and reaction of *n*-butyltin trichloride with the silver salt of the phosphinic acid, **1** and **2** were formed only by the former reaction (eq 1). The former reaction

$$4\,n\text{-BuSn(O)OH} + 4\text{R}_2\text{PO}_2\text{H} \rightarrow [n\text{-BuSn(O)O}_2\text{PR}_2]_4 + 4\text{H}_2\text{O} \quad (1)$$

$$\text{R} = t\text{-Bu (1)}, \text{CH}_2\text{Ph (2)}$$

has been used to prepare open-drum oxotin compounds[8,9] con-

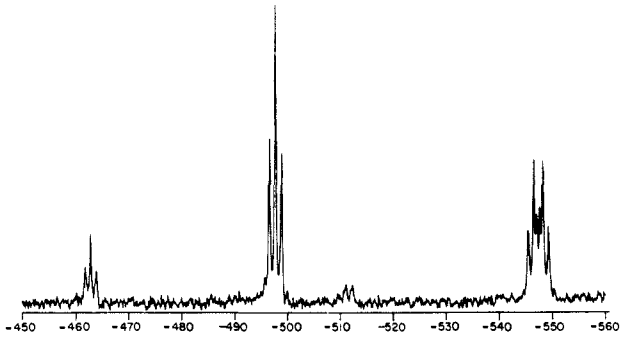

Figure 7. ^{119}Sn NMR spectrum ($CDCl_3$ solution) of a reaction product of *n*-butylstannoic acid with dicyclohexylphosphinic acid in a 1:1.5 molar ratio, respectively. The three resonance patterns with increasing shielding are the cube **5**, at −462.8 ppm, the O-capped cluster **4**, at −499.5 ppm, and the butterfly formulation **3**, at −547.5 ppm.

taining carboxylate ligands and a crown cluster with phosphinate ligands.[19] The condensation reaction of stannoic acid with phosphinic acid in forming the cubic structures, **1** and **2**, requires a 1:1 stoichiometry (eq 1), whereas this reaction leading to the butterfly cluster, **3**, proceeds in a 1:2 stoichiometric ratio of tin acid to phosphorus acid (eq 2). The drum composition $[R'Sn(O)O_2P(OR)_2]_6$ also results from a 1:1 reaction of tin acid to phosphorus-based acids.[1b]

$$2\,n\text{-BuSn(O)OH} + 4(C_6H_{11})_2PO_2H \rightarrow [n\text{-BuSn(OH)}(O_2P(C_6H_{11})_2)_2]_2 + 2H_2O \quad (2)$$

One may question then what favors the cube over the drum formulation. As previously discussed,[1b,4] the cube geometry offers greater accommodation for larger groups attached to the phosphinate ligand. The only drums prepared thus far with a phosphorus-based acid are $[n\text{-BuSn(O)}O_2P(OPh)_2]_6$ and the mixed-drum species, $[(MeSn(O)O_2CMe)(MeSn(O)O_2P(t\text{-Bu})_2)]_3$.[1b] The alteration in ligand type around the outside of the drum in the latter structure presumably allows the relaxation of any steric effect from the di-*tert*-butylphosphinate ligands. In the former drum configuration, the diphenyl phosphate ligands are of lesser steric requirement compared to the corresponding phosphinic acid since the phenyl groups are moved further out from the skeletal framework by the P–O bonding arrangement. It is reasonable that derivatives with all carboxylate ligands have not yielded any cubic arrays.[8,9] Here, steric effects should be minimal between carboxylate groups due to the presence of only one R group and the near planarity associated with the RCO_2 unit. Instead, a competition arises between drum and open-drum forms leading to reversible equilibria.[9]

In the present case with phosphinate ligands, interconversions of a different kind are found. Although the cube **1**, containing the di-*tert*-butylphosphinate ligands (depicted in Figures 1 and 2), exists in stable form in solution, both the cube **2** and butterfly **3** undergo transformations with adventitious water. The hydrolysis of **3** proceeds more slowly than that for **2**. Both yield an oxygen-capped cluster as demonstrated by their $CDCl_3$ solution-state ^{119}Sn and ^{31}P NMR spectra. For the cube **2**, a new triplet appeared at −499.2 ppm in the ^{119}Sn spectrum and increased in intensity at the expense of the triplet at −464.4 ppm. The ^{31}P NMR spectrum behaves similarly. The ^{119}Sn chemical shift is especially diagnostic of the type of structure present. As Table VII indicates, each formulation falls in a rather narrow chemical shift range with no overlap between ranges. Also, an interesting relation is noted in this table between increasing ^{119}Sn chemical shift and increasing ratio of stannoic acid to ligand acid for the various compositions.

Figure 7 shows a ^{119}Sn NMR spectrum of a reaction mixture of *n*-butylstannoic acid with dicyclohexylphosphinic acid in $CDCl_3$. The cube **5**, low-field triplet at −462.8 ppm, the O-capped cluster **4**, higher field triplet at −499.5 ppm, and the butterfly cluster **3**, highest field doublet of triplets at −547.5 ppm, are readily identified with reference to Table VII. As can be seen from Figure 7, the butterfly derivative **3** is formed in significant quantities, although the yield of the isolated pure product is very low. Of course, in this case, the cube **5** and butterfly cluster **3** were independently synthesized and have had their X-ray structures determined, **5** reported earlier[4] and **3** here.

The conversion of **3** to **4** is illustrated by the ^{31}P NMR spectra in Figure 8 obtained in less than 1 h after solution preparation and also after 6 days. The two types of phosphinate signals with ^{119}Sn satellites for the butterfly **3**, resonating at 56.0 and 47.6 ppm (1:1 intensity), decrease in intensity as the ^{31}P signal, with ^{119}Sn

Table II. Selected Distances (Å) and Angles (deg) for $[n\text{-BuSn(O)}O_2P(t\text{-Bu})_2]_4$ (**1**)[a]

	Distances		
Sn1–O1	2.069 (4)	Sn3–O31	2.139 (4)
Sn1–O2	2.139 (5)	Sn3–C301	2.152 (7)
Sn1–O4	2.144 (4)	Sn4–O1	2.132 (4)
Sn1–O11	2.147 (4)	Sn4–O3	2.142 (5)
Sn1–O42	2.131 (6)	Sn4–O4	2.057 (4)
Sn1–C101	2.164 (7)	Sn4–O32	2.159 (4)
Sn2–O1	2.137 (6)	Sn4–O41	2.149 (6)
Sn2–O2	2.071 (4)	Sn4–C401	2.167 (7)
Sn2–O3	2.133 (4)	O11–P1	1.527 (6)
Sn2–O12	2.142 (4)	O12–P1	1.531 (5)
Sn2–O21	2.141 (6)	O21–P2	1.526 (5)
Sn2–C201	2.144 (7)	O22–P2	1.519 (6)
Sn3–O2	2.131 (4)	O31–P3	1.531 (6)
Sn3–O3	2.073 (4)	O32–P3	1.521 (5)
Sn3–O4	2.135 (5)	O41–P4	1.534 (4)
Sn3–O22	2.153 (6)	O42–P4	1.525 (5)
	Angles		
O1–Sn1–O2	80.4 (2)	O4–Sn3–C301	99.7 (3)
O1–Sn1–O4	80.1 (1)	O22–Sn3–O31	94.7 (2)
O1–Sn1–O11	85.9 (2)	O22–Sn3–C301	93.3 (3)
O1–Sn1–O42	86.2 (2)	O31–Sn3–C301	94.1 (2)
O1–Sn1–C101	178.1 (2)	O1–Sn4–O3	80.0 (2)
O2–Sn1–O4	80.0 (2)	O1–Sn4–O4	80.6 (2)
O2–Sn1–O11	91.7 (2)	O1–Sn4–O32	164.0 (2)
O2–Sn1–O42	165.0 (1)	O1–Sn4–O41	90.4 (2)
O2–Sn1–C101	98.3 (3)	O1–Sn4–C401	100.6 (2)
O4–Sn1–O11	164.7 (2)	O3–Sn4–O4	80.4 (2)
O4–Sn1–O42	91.1 (2)	O3–Sn4–O32	90.2 (2)
O4–Sn1–C101	98.4 (2)	O3–Sn4–O41	164.6 (1)
O11–Sn1–O42	94.1 (2)	O3–Sn4–C401	100.9 (3)
O11–Sn1–C101	95.5 (2)	O4–Sn4–O32	85.4 (2)
O42–Sn1–C101	94.9 (3)	O4–Sn4–O41	86.2 (2)
O1–Sn2–O2	80.4 (2)	O4–Sn4–C401	178.2 (3)
O1–Sn2–O3	80.1 (2)	O32–Sn4–O41	96.4 (2)
O1–Sn2–O12	90.7 (2)	O32–Sn4–C401	93.5 (2)
O1–Sn2–O21	164.6 (2)	O41–Sn4–C401	92.5 (3)
O1–Sn2–C201	101.2 (3)	Sn1–O1–Sn2	98.8 (2)
O2–Sn2–O3	80.5 (1)	Sn1–O1–Sn4	98.8 (2)
O2–Sn2–O12	84.8 (2)	Sn2–O1–Sn4	99.5 (2)
O2–Sn2–O21	85.9 (2)	Sn1–O2–Sn2	98.7 (2)
O2–Sn2–C201	177.8 (3)	Sn1–O2–Sn3	99.3 (2)
O3–Sn2–O12	163.8 (2)	Sn2–O2–Sn3	98.8 (1)
O3–Sn2–O21	90.7 (2)	Sn2–O3–Sn3	98.6 (1)
O3–Sn2–C201	101.2 (2)	Sn2–O3–Sn4	99.3 (2)
O12–Sn2–O21	95.1 (2)	Sn3–O3–Sn4	98.5 (2)
O12–Sn2–C201	93.6 (2)	Sn1–O4–Sn3	99.0 (2)
O21–Sn2–C201	92.7 (3)	Sn1–O4–Sn4	98.8 (2)
O2–Sn3–O3	80.5 (1)	Sn3–O4–Sn4	99.2 (2)
O2–Sn3–O4	80.4 (2)	Sn1–O11–P1	129.3 (3)
O2–Sn3–O22	90.2 (2)	Sn2–O12–P1	131.1 (3)
O2–Sn3–O31	164.7 (2)	Sn2–O21–P2	130.6 (3)
O2–Sn3–C301	100.1 (2)	Sn3–O22–P2	129.7 (3)
O3–Sn3–O4	80.2 (2)	Sn3–O31–P3	129.8 (3)
O3–Sn3–O22	86.8 (2)	Sn4–O32–P3	130.3 (3)
O3–Sn3–O31	85.3 (2)	Sn4–O41–P4	130.3 (3)
O3–Sn3–C301	179.4 (2)	Sn1–O42–P4	130.6 (3)
O4–Sn3–O22	165.0 (2)		
O4–Sn3–O31	91.7 (2)		

[a] Estimated standard deviations in parentheses. The atom-labeling scheme is shown in Figures 1 and 2.

(19) Kumara Swamy, K. C.; Schmid, C. G.; Day, R. O.; Holmes, R. R. *J. Am. Chem. Soc.*, following paper in this issue.

Table III. Atomic Coordinates in Crystalline $[n\text{-BuSn(O)O}_2\text{P(CH}_2\text{Ph)}_2]_4$ (**2**)[a]

atom[b]	x	y	z	B_{eq}[c]	atom[b]	x	y	z	B_{eq}[c]
Sn	0.00875 (3)	0.09164 (3)	0.09472 (5)	3.36 (1)	C14	−0.2400 (8)	0.3939 (6)	0.215 (1)	6.7 (3)
P	−0.1603 (1)	0.1580 (1)	0.0344 (2)	3.66 (5)	C15	−0.1739 (9)	0.4330 (7)	0.211 (1)	7.6 (4)
O1	0.0067 (3)	0.0788 (3)	−0.0793 (5)	3.4 (1)	C16	−0.1150 (8)	0.4117 (6)	0.140 (1)	6.8 (3)
O11	−0.0772 (3)	0.1754 (4)	0.0672 (6)	4.2 (1)	C17	−0.1275 (6)	0.3528 (6)	0.072 (1)	5.5 (3)
O12	−0.1678 (4)	0.1005 (4)	−0.0626 (5)	4.1 (1)	C21	−0.2099 (5)	0.1245 (6)	0.1585 (9)	4.5 (2)
C1	0.0141 (8)	0.1077 (7)	0.2762 (8)	6.5 (3)	C22	−0.2953 (5)	0.1165 (5)	0.1487 (8)	3.8 (2)
C2	−0.002 (1)	0.189 (1)	0.308 (2)	11.4 (5)*	C23	−0.3297 (6)	0.0810 (6)	0.056 (1)	5.5 (3)
C3	−0.015 (1)	0.198 (1)	0.444 (2)	13.6 (7)*	C24	−0.4076 (6)	0.0725 (7)	0.050 (1)	6.8 (3)
C4	0.044 (1)	0.182 (2)	0.510 (2)	15.3 (8)*	C25	−0.4511 (6)	0.1015 (7)	0.141 (1)	6.4 (3)
C11	−0.2069 (5)	0.2444 (5)	−0.0105 (9)	4.2 (2)	C26	−0.4190 (6)	0.1359 (7)	0.231 (1)	6.1 (3)
C12	−0.1947 (5)	0.3099 (5)	0.0721 (8)	4.0 (2)	C27	−0.3404 (6)	0.1443 (6)	0.2339 (9)	5.2 (2)
C13	−0.2523 (7)	0.3299 (6)	0.1440 (9)	5.5 (3)					

[a] Numbers in parentheses are estimated standard deviations. [b] Atoms are labeled to agree with Figure 3. [c] Equivalent isotropic thermal parameters are calculated as $^4/_3[a^2\beta_{11} + b^2\beta_{22} + c^2\beta_{33} + ab(\cos\gamma)\beta_{12} + ac(\cos\beta)\beta_{13} + bc(\cos\alpha)\beta_{23}]$.

Table IV. Selected Distances (Å) and Angles (deg) for $[n\text{-BuSn(O)O}_2\text{P(CH}_2\text{Ph)}_2]_4$ (**2**)[a]

	Distances		
Sn–O1	2.070 (5)	Sn–O12′	2.136 (6)
Sn–O1″	2.158 (6)	Sn–C1	2.17 (1)
Sn–O1′	2.136 (6)	O11–P	1.547 (7)
Sn–O11	2.140 (6)	O12–P	1.537 (7)
	Angles		
O1–Sn–O1″	80.1 (2)	O1′–Sn–O12′	93.3 (2)
O1–Sn–O1′	80.6 (2)	O1′–Sn–C1	99.5 (4)
O1–Sn–O11	85.0 (2)	O11–Sn–O12′	94.3 (2)
O1–Sn–O12′	84.6 (2)	O11–Sn–C1	95.2 (4)
O1–Sn–C1	178.1 (4)	O12′–Sn–C1	93.5 (4)
O1″–Sn–O1′	81.0 (2)	Sn–O1–Sn″	99.3 (2)
O1″–Sn–O11	87.7 (2)	Sn–O1–Sn′	98.6 (2)
O1″–Sn–O12′	164.3 (2)	Sn″–O1–Sn′	98.2 (2)
O1″–Sn–C1	101.9 (4)	Sn–O11–P	124.9 (4)
O1′–Sn–O11	162.9 (2)	Sn″–O12–P	125.3 (4)

[a] Estimated standard deviations in parentheses. The atom-labeling scheme is shown in Figure 3.

satellites indicative of the O-capped cluster **4**, grows in at 54.6 ppm. The ^{31}P resonance expected at 44.0 ppm for the phosphinate anion most likely is absent due to fast exchange with phosphinic acid released in the hydrolysis. This conversion proceeds to over 95%. The reactions generating the O-capped cluster follow eq 3 and 4 for **2** and **3**, respectively. In the former process, hydrolysis

$$[R'Sn(O)O_2PR_2]_4(\text{cube } \mathbf{2}\ (R' = Bu,\ R = CH_2Ph)) + 2H_2O \rightarrow [(R'Sn(OH)O_2PR_2)_3O][R_2PO_2](\text{O-capped cluster}) + R'Sn(O)OH \quad (3)$$

$$3[R'Sn(OH)(O_2PR_2)_2]_2(\text{butterfly } \mathbf{3}\ (R' = Bu,\ R = C_6H_{11})) + 2H_2O \rightarrow 2[(R'Sn(OH)O_2PR_2)_3O][R_2PO_2](\text{O-capped cluster } (\mathbf{4})) + 4R_2PO_2H \quad (4)$$

proceeds with the generation of stannoic acid, while in the latter hydrolysis, phosphinic acid is formed. Formation of phosphinic acid crystals were noted while preparing a suitable crystal of **3** for X-ray analysis. In any event, the ^{119}Sn and ^{31}P chemical shifts and coupling constants giving rise to the transformation indicated in Figure 8 correspond to the O-capped cluster (**4**), identified as such in the conversion of the dicyclohexyl cube **5** to this species. In accord with eq 3 and 4 then, the O-capped cluster arrangement is hydrolytically more stable than either the cube or butterfly compositions.

Structural Aspects. Although the idealized symmetry of the cube is D_{2d}, neither **1** nor **2** realizes this symmetry crystallographically. The asymmetric unit in **1** contains the entire molecule, while **2** has crystallographic S_4 symmetry. For **3**, halves of the dimer are related by a crystallographic inversion center, and thus the crystallographic symmetry, C_i, is the same as the idealized molecular symmetry.

While the structural motif Sn–O(H)–Sn–O(H) has been observed previously for hexacoordinated tin, **3** represents a new geometric form for tin compounds in that the four-membered [Sn–O–Sn–O] ring is spanned on both sides by symmetrical phosphinate bridges between the tin atoms. In addition to two bonds to bridging phosphinate ligands, two bonds to bridging hydroxide groups, and one bond to an *n*-butyl group, each tin atom has a sixth bond to a "dangling" phosphinate ligand. The monodentate nature of this ligand is reflected in the P–O bond lengths. The P–O21 distance (O21 bonded to Sn) is 1.547 (3) Å while the P–O22 distance is 1.488 (4) Å, reflecting P=O double bond character. The dangling oxygen, O22, is 1.885 Å from the hydrogen atom of the bridging hydroxyl group, which is indicative of a hydrogen bridging interaction (van der Waals sum of oxygen and hydrogen is 2.7 Å[20]).

Table V. Atomic Coordinates in Crystalline $[n\text{-BuSn(OH)(O}_2\text{P(C}_6\text{H}_{11})_2)_2]_2$ (**3**)[a]

atom[b]	x	y	z	B_{eq}[c]	atom[b]	x	y	z	B_{eq}[c]
Sn	0.05655 (3)	−0.04611 (2)	0.10304 (2)	3.873 (6)	C21	0.3242 (6)	−0.1140 (5)	−0.2195 (5)	7.9 (1)
P1	0.2609 (1)	−0.0020 (1)	−0.1450 (1)	4.68 (3)	C22	0.4270 (6)	−0.1794 (5)	−0.1784 (6)	8.6 (2)
P2	−0.0162 (1)	−0.31476 (9)	0.18756 (9)	3.97 (2)	C23	0.4830 (9)	−0.2728 (7)	−0.2474 (8)	13.7 (3)
O1	−0.0143 (3)	−0.1036 (2)	−0.0090 (2)	4.12 (6)	C24	0.3950 (8)	−0.3304 (6)	−0.2765 (9)	13.3 (3)
O11	0.2315 (3)	−0.0434 (3)	−0.0223 (3)	5.05 (7)	C25	0.2952 (8)	−0.2607 (6)	−0.3239 (6)	9.1 (2)
O12	0.1479 (3)	0.0458 (3)	−0.1858 (3)	4.85 (7)	C26	0.2309 (7)	−0.1793 (6)	−0.2436 (7)	11.8 (2)
O21	0.0710 (3)	−0.2095 (2)	0.1743 (2)	4.21 (6)	C31	−0.1165 (5)	−0.3335 (4)	0.3274 (4)	5.0 (1)
O22	−0.0980 (3)	−0.3055 (2)	0.1116 (3)	4.94 (7)	C32	−0.2244 (5)	−0.4245 (5)	0.3602 (5)	6.1 (1)
C1	0.1336 (6)	0.0346 (5)	0.2052 (4)	7.4 (1)	C33	−0.3122 (6)	−0.4214 (7)	0.4745 (6)	8.5 (2)
C2	0.1381 (9)	−0.0210 (7)	0.3085 (6)	12.3 (2)	C34	−0.2400 (6)	−0.4331 (6)	0.5562 (5)	8.5 (2)
C3	0.198 (1)	0.0524 (8)	0.3696 (6)	13.4 (2)	C35	−0.1324 (7)	−0.3479 (6)	0.5250 (5)	8.7 (2)
C4	0.221 (1)	−0.003 (1)	0.463 (1)	19.8 (5)	C36	−0.0390 (6)	−0.3483 (5)	0.4106 (4)	6.7 (1)
C11	0.3928 (6)	0.1037 (5)	−0.1802 (5)	7.2 (1)	C41	0.0968 (4)	−0.4278 (3)	0.1702 (4)	4.6 (1)
C12	0.4300 (6)	0.1620 (5)	−0.2967 (5)	6.8 (1)	C42	0.2077 (5)	−0.3970 (5)	0.0712 (5)	6.6 (2)
C13	0.5384 (7)	0.2530 (7)	−0.3233 (6)	9.4 (2)	C43	0.3067 (6)	−0.4909 (5)	0.0616 (6)	7.7 (2)
C14	0.5575 (9)	0.2992 (8)	−0.2417 (8)	16.0 (3)	C44	0.2425 (6)	−0.6000 (5)	0.0607 (5)	7.5 (2)
C15	0.5235 (6)	0.2376 (6)	−0.1260 (5)	8.9 (2)	C45	0.1279 (8)	−0.6322 (5)	0.1563 (6)	9.1 (2)
C16	0.4011 (8)	0.1566 (7)	−0.0966 (6)	12.7 (2)	C46	0.0300 (6)	−0.5372 (4)	0.1680 (6)	7.4 (2)

[a] Numbers in parentheses are estimated standard deviations. [b] Atoms are labeled to agree with Figures 5 and 6. [c] Equivalent isotropic thermal parameters are calculated as $^4/_3[a^2\beta_{11} + b^2\beta_{22} + c^2\beta_{33} + ab(\cos\gamma)\beta_{12} + ac(\cos\beta)\beta_{13} + bc(\cos\alpha)\beta_{23}]$.

Table VI. Selected Distances (Å) and Angles (deg) for $[n\text{-BuSn(OH)}(O_2P(C_6H_{11})_2)_2]_2$ (3)[a]

	Distances		
Sn-O1	2.047 (3)	Sn-C1	2.123 (7)
Sn-O1′	2.128 (3)	O11-P1	1.533 (4)
Sn-O11	2.115 (3)	O12-P1	1.530 (4)
Sn-O12′	2.162 (3)	O21-P2	1.547 (3)
Sn-O21	2.061 (3)	O22-P2	1.488 (4)
O1-H1	0.898	H1-O22	1.885
	Angles		
O1-Sn-O1′	76.8 (1)	O11-Sn-O21	94.4 (1)
O1-Sn-O11	80.9 (1)	O11-Sn-C1	96.6 (2)
O1-Sn-O12′	81.6 (1)	O12′-Sn-O21	92.7 (1)
O1-Sn-O21	89.3 (1)	O12′-Sn-C1	99.8 (2)
O1-Sn-C1	172.3 (2)	O21-Sn-C1	98.1 (2)
O1′-Sn-O11	86.6 (1)	Sn-O1-Sn′	103.2 (1)
O1′-Sn-O12′	82.4 (1)	Sn-O11-P1	130.2 (2)
O1′-Sn-O21	165.8 (1)	Sn′-O12-P1	130.8 (2)
O1′-Sn-C1	95.9 (2)	Sn-O21-P2	130.1 (2)
O11-Sn-O12′	161.0 (1)		

[a] Estimated standard deviations in parentheses. The atom-labeling scheme is shown in Figures 5 and 6.

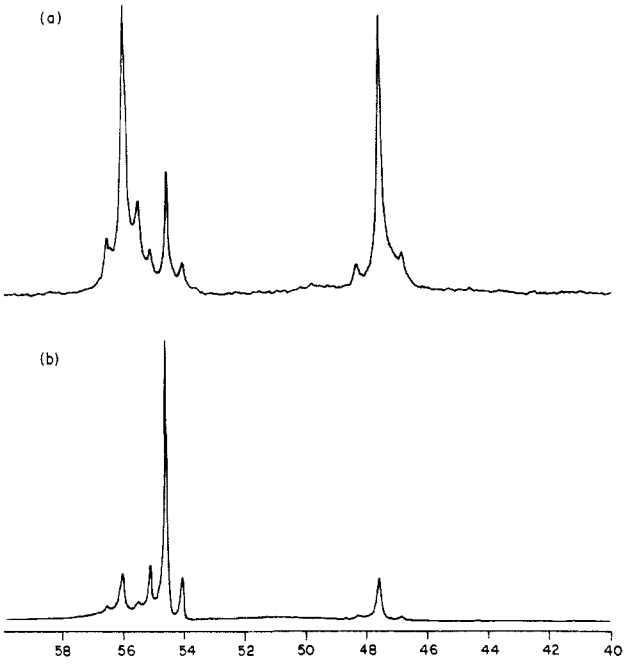

Figure 8. ^{31}P NMR spectrum ($CDCl_3$ solution) of the same reaction product as in Figure 7 (a) obtained in less than 1 h after sample preparation showing two equal intensity triplets at 56.0 ppm (bridging phosphinate) and at 47.6 ppm (dangling phosphinate) corresponding to the butterfly 3 and a low-intensity triplet at 54.6 ppm associated with the cation of the *o*-capped cluster 4 and (b) obtained after 6 days showing the growth of the O-capped triplet at 54.6 ppm and the diminished intensity due to the two triplets arising from the butterfly 3.

The structural relation between a drum and an O-capped cluster has been discussed.[5] Since the construction of the cube is closer than the drum to that of the O-capped cluster, the cube transformation to the latter geometry should be easier to visualize. The basic framework of the O-capped cluster is that of a cube with with a corner missing. In a formalistic sense, an R-Sn ligand unit must be removed from the cube and yield a stannoic acid molecule. Accompanying this removal, ligand rearrangement is necessary, resulting in the formation of the phosphinate anion. With the formal addition of hydrogen atoms from water molecules to form the hydroxyl groups, an O-capped cluster is obtained from a cube. Mechanistically, however, no information is available on the detailed steps in the conversion or on whether it is possible to isolate any intermediate formations.

Consideration of the hydrolysis process in eq 4 and the framework for the butterfly illustrated for 3 in Figure 5 shows it is unclear, even formally, to understand how three molecules of 3 yield two molecules of the corresponding O-capped cluster 4. Even so, comparison of the skeletal structures (Figure 9) shows a major component of the butterfly unit is contained in the framework of the O-capped cluster.

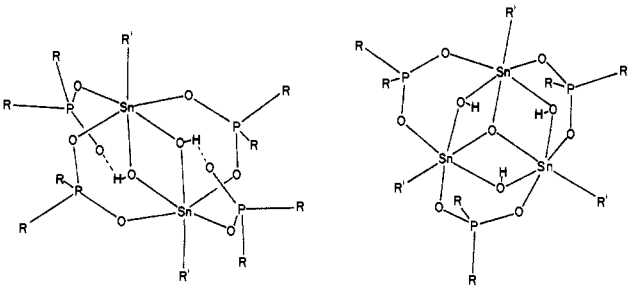

Figure 9. Skeletal representations showing the structural relations between the butterfly (left) and oxygen-capped cluster (right).

Table VII. ^{119}Sn Chemical Shifts for *n*-Butyloxotin Clusters in $CDCl_3$[a]

cluster[b]	av δ[c]	Sn/ligand[d]	H_2O/Sn[e]	ref
cube (3)	−466.1 ± 4.7	1	1	4, this work
drum (6)	−487.9 ± 1.8	1	1	1b, 7
crown (2)	−525.4 ± 10	4/5	1/2	19
O-capped (4)	−501.1 ± 3.9	3/4	2/3	1b, 5, this work
ladder (5)	−523.5 ± 2.2 −549.4 ± 2.8 −621.9 ± 10.7	3/5	4/3	7, 8
butterfly (1)	−547.4	1/2	1	this work
extended (1)	−575			
	−614	2/5	3/2	19

[a] Summarized here are ^{119}Sn chemical shifts for clusters containing mainly phosphinate and carboxylate ligands. Recent unpublished work in our laboratory with arsenic ligands shows that the ^{119}Sn chemical shifts for the tin clusters depend on the ligand attachment in the order: arsinate < phosphinate < phosphate. [b] Number in parentheses represents number of compounds studied. [c] All in $CDCl_3$ except the cube $[n\text{-BuSn(O)O}_2\text{P}(tert\text{-Bu})_2]_4$, which was studied in C_6D_6. [d] Mole ratio of the stoichiometric amount of the organostannoic acid in reaction with the ligand acid. [e] Mole ratio of water formed to stannoic acid used in the condensation reaction of stannoic acid with ligand acid.

Acknowledgment. The support of this research by the National Science Foundation, Grant CHE-8504737, and the donors of the Petroleum Research Fund, administered by the American Chemical Society, is gratefully acknowledged.

Registry No. 1, 116052-69-8; 2, 116052-70-1; 3, 116076-45-0; 4, 116076-48-3; 5, 109890-41-7; *n*-BuSn(O)OH, 2273-43-0; *A*-Bu_2PO_2H, 677-76-9; $(PhCH_2)_2PO_2H$, 7369-51-9; $(C_6H_{11})_2PO_2H$, 832-39-3; ^{119}Sn, 14314-35-3; *n*-butyltin trichloride silver dicycloehxylphosphinate, 1118-46-3.

Supplementary Material Available: Listings of anisotropic thermal parameters (Table S1) and additional bond lengths and angles (Table S2) for 1 and anisotropic thermal parameters, hydrogen atom parameters, and additional bond lengths and angles (Tables S3–S5, respectively, for 2 and Tables S6–S8, respectively, for 3) (19 pages); tables of calculated and observed structure factors (56 pages). Ordering information is given on any current masthead page.

(20) Bondi, A. *J. Phys. Chem.* **1964**, *68*, 441–456.